

Electronic Supplementary Information for

**Effective Oxygen Activation on Polyoxometalate-based Hybrids for  
Epoxidation of Alkenes**

Xue Bai, Maochun Zhu, Yifei Liu, Min Xing, Xiaoying Ji, Ange Zhang, Yanli Yang, Ying Lu,  
Shuxia Liu\*

Key Laboratory of Polyoxometalate and Reticular Material Chemistry of Ministry of Education,  
College of Chemistry, Northeast Normal University, Changchun 130024, China. E-mail:  
liusx@nenu.edu.cn.

## Content

### 1. Experimental Section

1.1 Materials and Instrumentation

1.2 Synthesis of  $[\text{Co}(\text{btap})_3(\text{H}_2\text{O})_3(\text{HPW}_{12}\text{O}_{40})] \cdot 3\text{H}_2\text{O}$  (**Co-PW**).

1.3 Synthesis of  $[\text{Mn}(\text{btap})_3(\text{H}_2\text{O})_3(\text{HPW}_{12}\text{O}_{40})] \cdot 3.5\text{H}_2\text{O}$  (**Mn-PW**).

1.4 Catalytic epoxidation of styrene and its derivatives over  $\text{O}_2$ / IBA system.

### 2. Crystallography

**Table S1** Crystal data and structure refinement for the compounds **Co-PW** and **Mn-PW**.

**Table S2** Selected bond distances (Å) and angles (°) for the title compounds **Co-PW** and **Mn-PW**.

**Table S3** Selected hydrogen-bonding geometry (Å, °) for compound **Co-PW**.

**Table S4** The Bond-Valence Sum Calculations for the tungsten ions and cobalt ions in **Co-PW**.

**Table S5** The Bond-Valence Sum Calculations for the tungsten ions and manganese ions in **Mn-PW**.

**Fig. S1** Coordination mode of Mn (II) ion of **Mn-PW**.

**Fig. S2** The PXRD patterns of compounds **Co-PW** and **Mn-PW**.

**Fig. S3** The FT-IR spectrums of compounds **Co-PW** and **Mn-PW**.

**Fig. S4** TG-DTG curves of compounds **Co-PW** and **Mn-PW**.

**Fig. S5** The XPS spectrum of compound **Co-PW**.

**Fig. S6** PXRD patterns of compounds **Co-PW** and **Mn-PW** after immersing in a series of common solvents for 7 days and in different acid/base solutions with a pH of 1-13.

**Fig. S7** BET analysis of compounds **Co-PW** and **Mn-PW**.

**Fig. S8.** DLS data for compounds **Co-PW** and **Mn-PW**.

**Table S6** Conversion and Selectivity of the Oxidation of Styrene to Styrene Oxide by compound **Co-PW** with  $\text{O}_2$  as the Oxidant.

**Fig. S9** Styrene conversion over **Co-PW** in the presence of the different trapping species.

**Table S7** Comparison of different catalysts on styrene epoxidation

## 1. Experimental Section

### 1.1 Materials and Instrumentation

All starting materials, reagents and solvents purchased commercially were used without purification in the experiments. The  $\text{H}_3\text{PW}_{12}\text{O}_{40}$  was prepared in the light of the literature method.<sup>1</sup> Powder X-ray diffraction (PXRD) measurements were performed on a SmartLab instrument with Cu  $\text{K}\alpha$  ( $\lambda = 1.5418 \text{ \AA}$ ) radiation and X-ray 40 kV/ 30 mA over the angular range  $2\theta 5^\circ - 50^\circ$  at a scan rate of  $10^\circ \text{ min}^{-1}$ . The Fourier transform infrared (FTIR) spectra were collected on NICOLET iS50 FT-IR spectrophotometer in the range  $400\text{-}4000 \text{ cm}^{-1}$ . The C, H and N elemental analysis were conducted on a Perkin-Elmer 2400 CHN elemental analyzer. Elemental analyses for P, W, Co, and Mn were obtained using a Prodigy inductively coupled plasma atomic emission spectrometry (ICP-AES) emission spectrometer. Thermogravimetric (TG) analyses were performed on a TA SDT Q600 TG instrument at a heating rate of  $10 \text{ }^\circ\text{C min}^{-1}$  from 25 to  $800 \text{ }^\circ\text{C}$  in nitrogen atmosphere. The conversion and selectivity of catalytic reaction was analyzed by using an Agilent Technologies 7820A gas chromatograph with a flame ionization detector equipped with a HP-5 column. The olefin oxidation products were identified with GC-MS and quantified using gas chromatography with internal standard techniques. Diameter and diameter distribution of the nanoparticles were determined by a Malvern Zetasizer Nano instrument for dynamic light scattering (DLS). Nitrogen adsorption/desorption measurement was taken by Autosorb-iQ instrument at 77K.

### 1.2 Synthesis of $[\text{Co}(\text{btap})_3(\text{H}_2\text{O})_3(\text{HPW}_{12}\text{O}_{40})] \cdot 3\text{H}_2\text{O}$ (Co-PW).

The mixture of  $\text{CoCl}_2$  (0.15 mmol, 0.04 g), btap (0.05 mmol, 0.01 g), and  $\text{H}_3\text{PW}_{12}\text{O}_{40}$  (0.05 mmol, 0.15 g) was dissolved in 8.0 mL  $\text{H}_2\text{O}$  with stirring the solution for 60 min, and then, the pH value of the mixture was adjusted to ca. 1.77 by 1 M HCl. The suspension was placed in a 23 mL Teflon-lined stainless steel reactor and kept heating at  $120 \text{ }^\circ\text{C}$  for 72 h. After cooling down to room temperature at the rate of  $10 \text{ }^\circ\text{C / h}$ , the pink block crystals could be obtained in 45% yield (based on W), and further collected by filtration, washed with deionized water, and dried. Anal. Calcd (%) for

$C_{18}H_{27}CoN_{14}O_{46}PW_{12}$  ( $M_r = 3471.63$ ): C, 6.23; H, 0.78; N, 5.65; Co, 1.70; P, 0.89; W, 63.55. Found (%): C, 6.21; H, 0.77; N, 5.62; Co, 1.67; P, 0.85; W, 63.54. IR (KBr,  $cm^{-1}$ ): 3439 (m), 3130 (w), 1607 (m), 1519 (s), 1485 (w), 1428 (w), 1365 (w), 1274 (s), 1226 (w), 1138 (m), 1077 (s), 975(s), 894 (m), 805 (s), 692 (w), 662 (m), 591 (w).

### 1.3 Synthesis of $[Mn(btap)_3(H_2O)_3(HPW_{12}O_{40})] \cdot 3.5H_2O$ (Mn-PW).

The synthesis of **Mn-PW** was similar to that of **Co-PW**, except that  $CoCl_2$  was replaced by  $MnCl_2$  (0.3 mmol, 0.06 g). The pH value was then adjusted to about 1.86 using 1.0 M HCl. After that obtained solution was transferred to a 23 mL Teflon-lined stainless steel reactor and heated at 140 °C for 72 h. The faint yellow crystals were generated by cooling to room temperature at the rate of 10 °C / h (yield: 40% based on W). Anal. Calcd (%) for  $C_{36}H_{56}Mn_2N_{28}O_{93}P_2W_{24}$  ( $M_r = 6953.30$ ): C, 6.22; H, 0.81; N, 5.64; Mn, 1.58; P, 0.89; W, 63.45. Found (%): C, 6.23; H, 0.78; N, 5.63; Mn, 1.55; P, 0.86; W, 63.41. IR (KBr,  $cm^{-1}$ ): 3428 (w), 3119 (m), 1606 (w), 1585 (w), 1514 (w), 1450 (m), 1428 (w), 1399 (w), 1358 (m), 1328 (m), 1280 (s), 1223 (m), 1136 (m), 1075 (s), 979 (s), 892 (s), 805 (s), 683 (w), 665 (m), 591 (w).

### 1.4 Catalytic epoxidation of styrene and its derivatives over $O_2$ /IBA system.

In a typical procedure, styrene (2 mmol), catalyst **Co-PW** (0.006 mmol, 20 mg), acetonitrile (5 mL), IBA (isobutyraldehyde, 4 mmol), and biphenyl (internal standard, 2 mmol) were first introduced into a 25 mL round-bottom flask equipped with a gas supply (oxygen purged through balloon), reflux condenser and magnetic stirrer. Then the mixture was stirred at 55 °C and sampled at different intervals during the reaction, which put into an ice chamber to stop the reaction. The conversion and selectivity were monitored by gas chromatography. The products were analyzed by GC-MS. A similar procedure was followed for the reusability tests that using styrene as the substrate. After the reaction, the reaction mixture was by centrifugation and filtration, and the catalyst was separated, washed with acetonitrile and ethanol, dried, and reused for the next run under the same conditions.

## 2. Crystallography

Single-crystal X-ray diffraction (SXRD) data of compounds **Co-PW** and **Mn-PW** were collected on a Bruker D8-Venture diffractometer using graphite-monochromated Mo K $\alpha$  radiation ( $\lambda = 0.71073 \text{ \AA}$ ) at 293 K.<sup>2</sup> The data were collected using the program APEX 3 and processed using the program SAINT routine in APEX 3. The empirical absorption correction was based on equivalent reflections. The structure was solved by direct methods and refined by full-matrix least-squares fitting on F<sup>2</sup> using Olex2 package and the SHELXL crystallographic software package.<sup>3-5</sup> Non-hydrogen atoms were refined with anisotropic displacement parameters during the final cycles. All hydrogen atoms of the organic molecule and water molecules were placed based on geometrical considerations and were included in the structure factor calculation. However the added H protons is not located in the crystal structure analysis, but were directly included in the final molecular formula. 2326146 and 2296918 contains the crystallographic data for compounds **Co-PW** and **Mn-PW**. The detailed crystallographic data for compounds **Co-PW** and **Mn-PW** are summarized in Table S1. Table S2 involves the selected bond lengths and angles.

**Table S1** Crystal data and structure refinement for the compounds **Co-PW** and **Mn-PW**.

Compound	<b>Co-PW</b>	<b>Mn-PW</b>
Empirical formula	C <sub>18</sub> H <sub>27</sub> CoN <sub>14</sub> O <sub>46</sub> PW <sub>12</sub>	C <sub>36</sub> H <sub>56</sub> Mn <sub>2</sub> N <sub>28</sub> O <sub>93</sub> P <sub>2</sub> W <sub>24</sub>
Formula weight	3471.63	6953.30
Temperature (K)	293	293
Wave length (Å)	0.71073	0.71073
Crystal system	Monoclinic	Monoclinic
Space group	<i>P2<sub>1</sub>/c</i>	<i>P2<sub>1</sub>/c</i>
<i>a</i> (Å)	13.0651(8)	13.1218(3)
<i>b</i> (Å)	18.4692(11)	18.3926(4)
<i>c</i> (Å)	23.0933(16)	23.5962(6)
$\alpha$ (°)	90	90
$\beta$ (°)	93.403(2)	93.494(2)
$\gamma$ (°)	90	90
Volume (Å <sup>3</sup> )	5562.6(6)	5684.2(2)
<i>Z</i>	4	2
<i>D<sub>c</sub></i> (mg cm <sup>-3</sup> )	4.144	4.061
$\mu$ (mm <sup>-1</sup> )	25.140	24.534
<i>F</i> (000)	6120	6132
Crystal size (mm <sup>3</sup> )	0.2 x 0.15 x 0.1	0.15 x 0.1 x 0.08
$\theta$ range (deg)	2.427 to 25.050	2.395 to 26.499
index range (deg)	-15 ≤ <i>h</i> ≤ 15, -21 ≤ <i>k</i> ≤ 21, -27 ≤ <i>l</i> ≤ 27	-15 ≤ <i>h</i> ≤ 16, -23 ≤ <i>k</i> ≤ 23, -29 ≤ <i>l</i> ≤ 29
Reflections collected	66938	83380
Unique reflections	9806	11775
<i>R</i> <sub>int</sub>	0.0853	0.0775
Data / restraints / parameters	9806 / 558 / 847	11775 / 133 / 851
GOF on <i>F</i> <sup>2</sup>	1.077	1.034
<i>R</i> <sub>1</sub> , <i>wR</i> <sub>2</sub> ( <i>I</i> > 2σ( <i>I</i> ))	0.0368, 0.0653	0.0497, 0.1087
<i>R</i> <sub>1</sub> , <i>wR</i> <sub>2</sub> (all data)	0.0602, 0.0728	0.0688, 0.1237
<sup>a</sup> $R_1 = \frac{\sum   F_o  -  F_c  }{\sum  F_o }$ , <sup>b</sup> $wR_2 = \frac{\sum [w(F_o^2 - F_c^2)^2]}{\sum [w(F_o^2)^2]}^{1/2}$		

**Table S2** Selected bond distances (Å) and angles (°) for the title compounds **Co-PW** and **Mn-PW**.

Compound <b>Co-PW</b>			
Co(1)-N(14)#1	2.092(11)	N(8)-Co(1)-O(1)	91.2(4)
Co(1)-N(8)	2.115(11)	N(8)-Co(1)-O(2)	89.7(5)
Co(1)-N(1)	2.138(10)	N(1)-Co(1)-O(1)	87.0(4)
Co(1)-O(3)	2.071(10)	N(1)-Co(1)-O(2)	165.2(5)
Co(1)-O(1)	2.147(9)	O(3)-Co(1)-N(14)#1	89.9(4)
Co(1)-O(2)	2.176(10)	O(3)-Co(1)-N(8)	83.3(4)
N(14)#1-Co(1)-N(8)	172.7(4)	O(3)-Co(1)-N(1)	104.0(4)
N(14)#1-Co(1)-N(1)	88.7(4)	O(3)-Co(1)-O(1)	167.7(4)
N(14)#1-Co(1)-O(1)	96.0(4)	O(3)-Co(1)-O(2)	90.7(5)
N(14)#1-Co(1)-O(2)	93.2(5)	O(1)-Co(1)-O(2)	78.2(5)
N(8)-Co(1)-N(1)	90.3(4)		
Symmetry codes for <b>Co-PW</b> : #1 x, -y+1/2, z-1/2.			
Compound <b>Mn-PW</b>			
Mn(1)-O(2)	2.135(14)	O(41)-Mn(1)-N(2)	85.8(6)
Mn(1)-O(41)	2.222(16)	O(43)-Mn(1)-O(41)	74.8(7)
Mn(1)-O(43)	2.210(16)	O(43)-Mn(1)-N(2)	160.5(7)
Mn(1)-N(7)	2.207(15)	N(7)-Mn(1)-O(41)	90.8(6)
Mn(1)-N(18)#1	2.200(16)	N(7)-Mn(1)-O(43)	92.4(8)
Mn(1)-N(2)	2.254(15)	N(18)#1-Mn(1)-O(41)	100.0(6)
O(2)-Mn(1)-O(41)	164.0(6)	N(18)#1-Mn(1)-O(43)	97.0(8)
O(2)-Mn(1)-O(43)	91.3(7)	N(18)#1-Mn(1)-N(2)	86.9(6)
O(2)-Mn(1)-N(2)	107.8(6)	N(18)#1-Mn(1)-N(7)	167.2(6)
O(2)-Mn(1)-N(7)	81.7(6)	N(7)-Mn(1)-N(2)	87.1(6)
O(2)-Mn(1)-N(18)#1	89.4(6)		
Symmetry codes for <b>Mn-PW</b> : #1 x, -y+1/2, z-1/2.			

**Table S3** Selected hydrogen-bonding geometry (Å, °) for compound **Co-PW**.

Compound	D–H⋯A	D–H	H⋯A	D⋯A	D–H⋯A
<b>Co-PW</b>	C(9)–H(9)⋯O(7)	0.93	2.47	3.1626	132
	C(12)–H(12)⋯O(12)	0.93	2.20	2.9871	142

**Table S4** The Bond-Valence Sum Calculations for the tungsten ions and cobalt ions in **Co-PW**.

Metal site	BVS cacl.	Assigned O.S	Metal site	BVS cacl.	Assigned O.S
W1	6.195	6	W8	6.282	6
W2	6.216	6	W9	6.134	6
W3	6.254	6	W10	6.155	6
W4	6.445	6	W11	6.221	6
W5	6.232	6	W12	6.296	6
W6	6.317	6	Co	1.884	2
W7	6.326	6			

**Table S5** The Bond-Valence Sum Calculations for the tungsten ions and manganese ions in **Mn-PW**.

Metal site	BVS cacl.	Assigned O.S	Metal site	BVS cacl.	Assigned O.S
W1	6.330	6	W8	6.197	6
W2	6.314	6	W9	6.234	6
W3	6.327	6	W10	6.276	6
W4	6.226	6	W11	6.118	6
W5	6.236	6	W12	6.391	6
W6	6.277	6	Mn	1.966	2
W7	6.125	6			

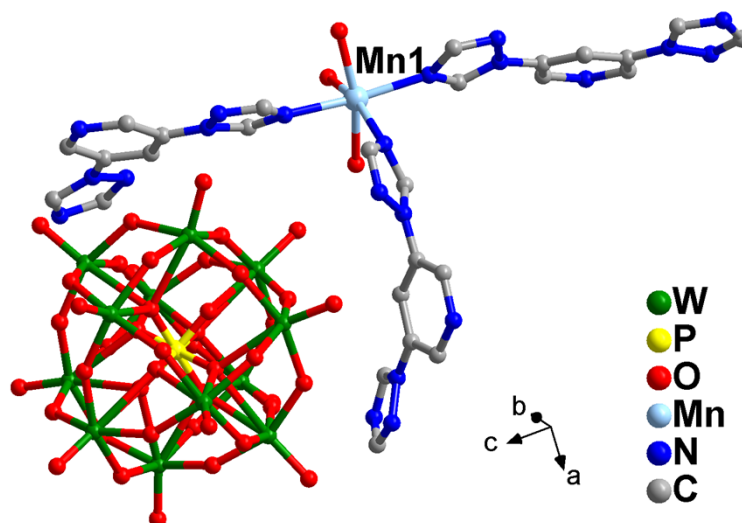


**Fig. S1** Coordination mode of Mn (II) ion of **Mn-PW**.

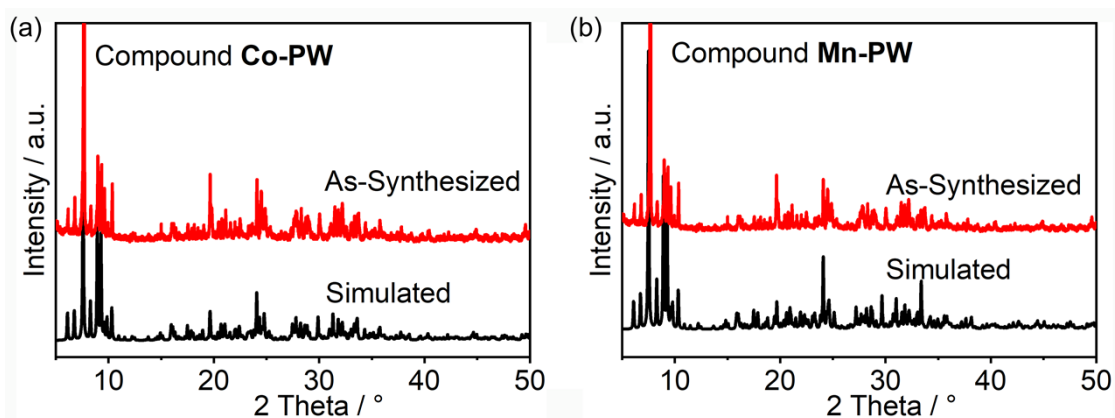


**Fig. S2** The PXRD patterns of compounds **Co-PW** and **Mn-PW**.

**PXRD Analyses.** The phase purity was first tested by powder X-ray diffraction (PXRD), which was shown in Fig. S2. The diffraction peaks of as synthesized compounds **Co-PW** and **Mn-PW** are consistent with their simulated ones, indicating that the obtained samples have high purity.

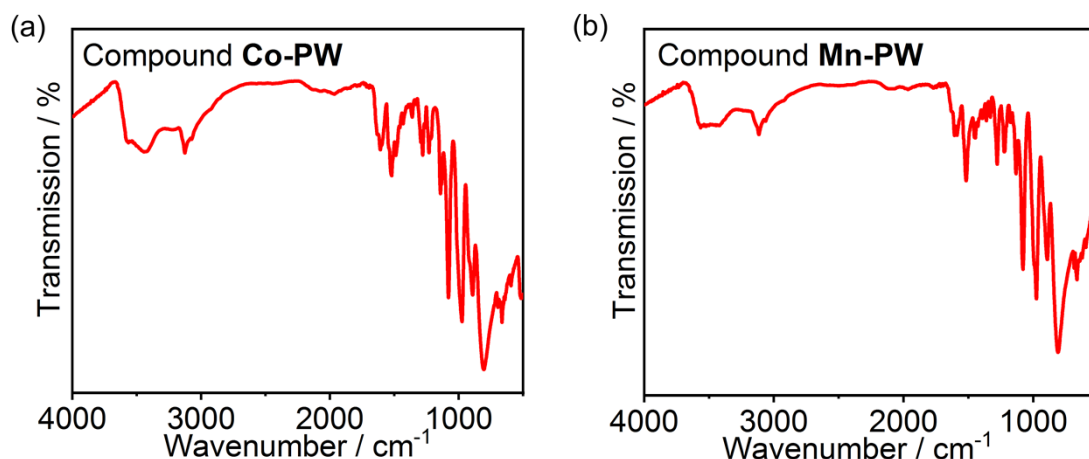


**Fig. S3** The FT-IR spectra of compounds **Co-PW** and **Mn-PW**.

**IR Analyses.** The FT-IR spectra of compounds **Co-PW** and **Mn-PW** were presented in Fig. S3. The strong peaks of  $1607\text{--}1428\text{ cm}^{-1}$  for **Co-PW**,  $1606\text{--}1428\text{ cm}^{-1}$  for **Mn-PW** can be assigned to the btap ligands.<sup>6,7</sup> The characteristic peaks at  $1077, 975, 894$  and  $805\text{ cm}^{-1}$  for **Co-PW**, and  $1075, 979, 892$  and  $805\text{ cm}^{-1}$  for **Mn-PW** show typical characteristic peaks of Keggin POM attributed to the  $\nu(\text{P-Oa})$ ,  $\nu(\text{W-Od})$ ,  $\nu(\text{W-Oc-W})$  and  $\nu(\text{W-Od-W})$ .<sup>8,9</sup> In addition, a broad band around  $3400\text{ cm}^{-1}$  and  $3100\text{ cm}^{-1}$  should be attributed to  $\nu(\text{O-H})$  of water molecules and  $\nu(\text{N-H})$  of organic ligands stretches.

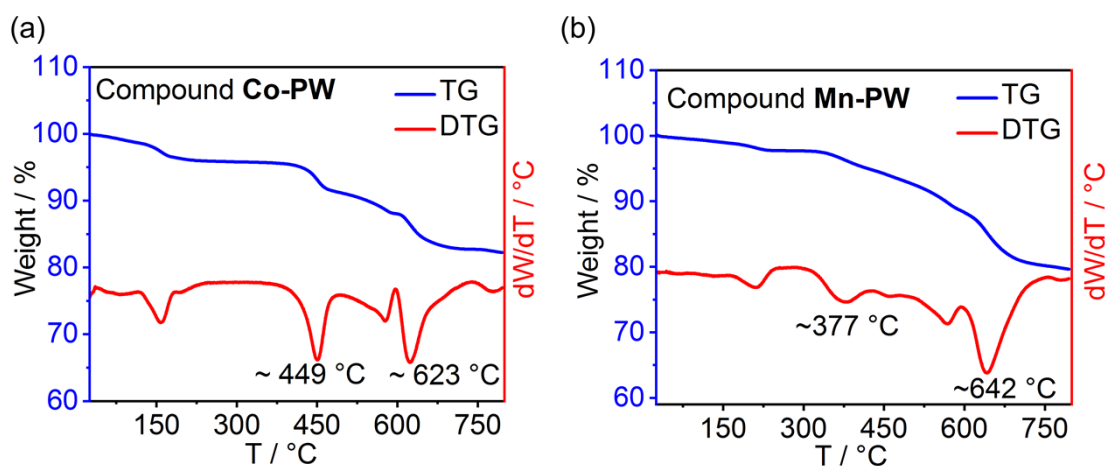


**Fig. S4** TG-DTG curves of compounds **Co-PW** and **Mn-PW**.

**TG Analyses.** As shown in Fig. S4, the thermal stability curves (TG-DTG) of **Co-PW** and **Mn-PW** exhibit two steps of weight loss: the first loss is 3.15 % at  $25\text{--}385\text{ °C}$  for

**Co-PW**, 3.36 % at 25–370 °C for **Mn-PW**, which corresponds to the loss of all water (calc. 3.11% for **Co-PW**, 3.32% for **Mn-PW**). And the second loss is 12.28 % (calc. 12.31%) at 390–670 °C for **Co-PW**, 12.26% (calc. 12.29%) at 370–660 °C for **Mn-PW** arising from the decomposition of the btap organic molecules. The total weight loss agrees with the calculated value for compounds **Co-PW** and **Mn-PW**. These results indicate that **Co-PW** and **Mn-PW** have very high thermal stability (stable at least below 370 °C).

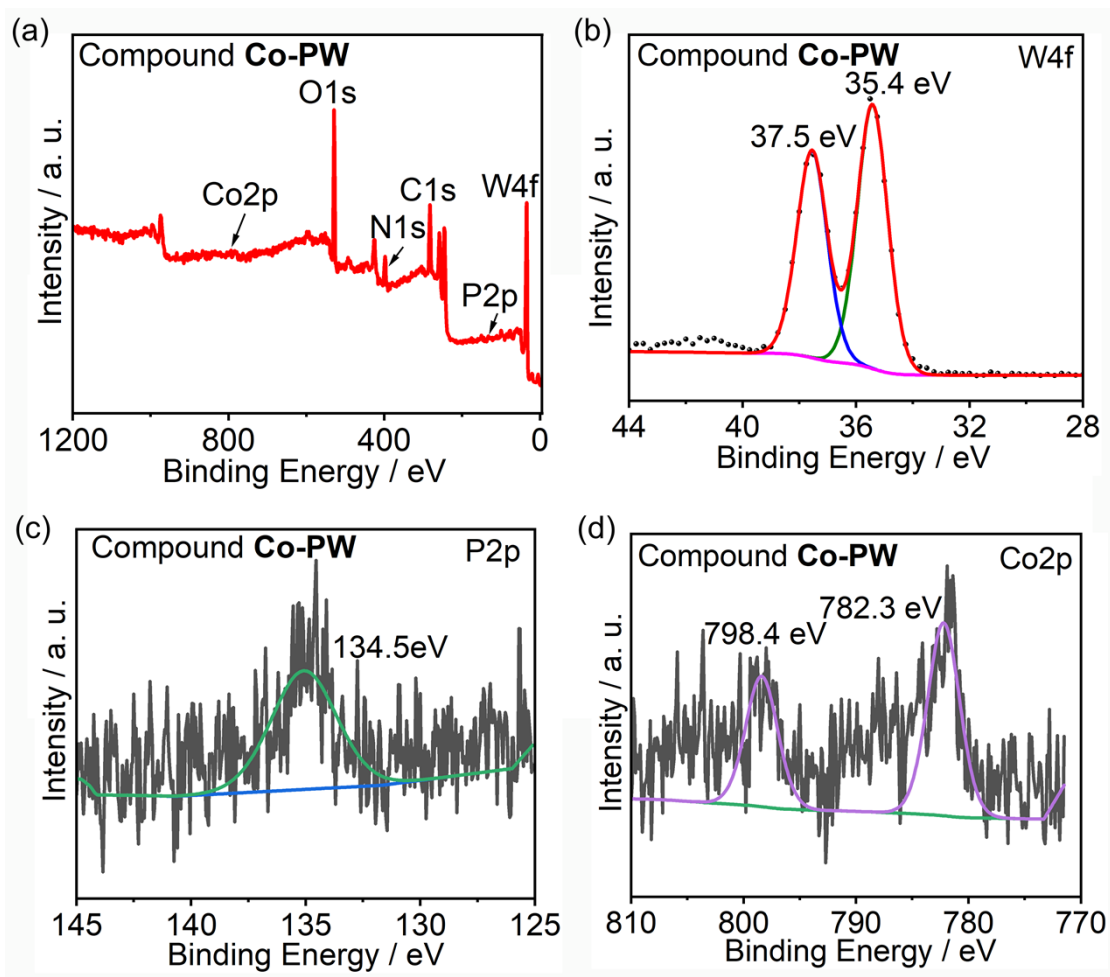


**Fig. S5** The XPS spectrum of compound **Co-PW**.

**XPS Analyses.** As shown in Fig. S5, the coexistence of W 4f, P 2p, O 1s, C 1s, N 1s, and Co 2p is detected in compound **Co-PW**. The peaks at 134.5 eV in compound **Co-PW**, can be classified as the characteristic peak of  $P^{5+}$ .<sup>10, 11</sup> The peaks at 35.4 and 37.5 eV in compound **Co-PW**, can be attributed to  $W 4f_{7/2}$  and  $W 4f_{5/2}$  of  $W^{6+}$ .<sup>12, 13</sup> The

peaks at 782.3 and 798.4 eV of compound **Co-PW**, may be assigned to the Co  $2p_{3/2}$  and Co  $2p_{1/2}$  of  $\text{Co}^{2+}$ .<sup>7, 14</sup> The results are consistent with the structural analyses and charge balance.

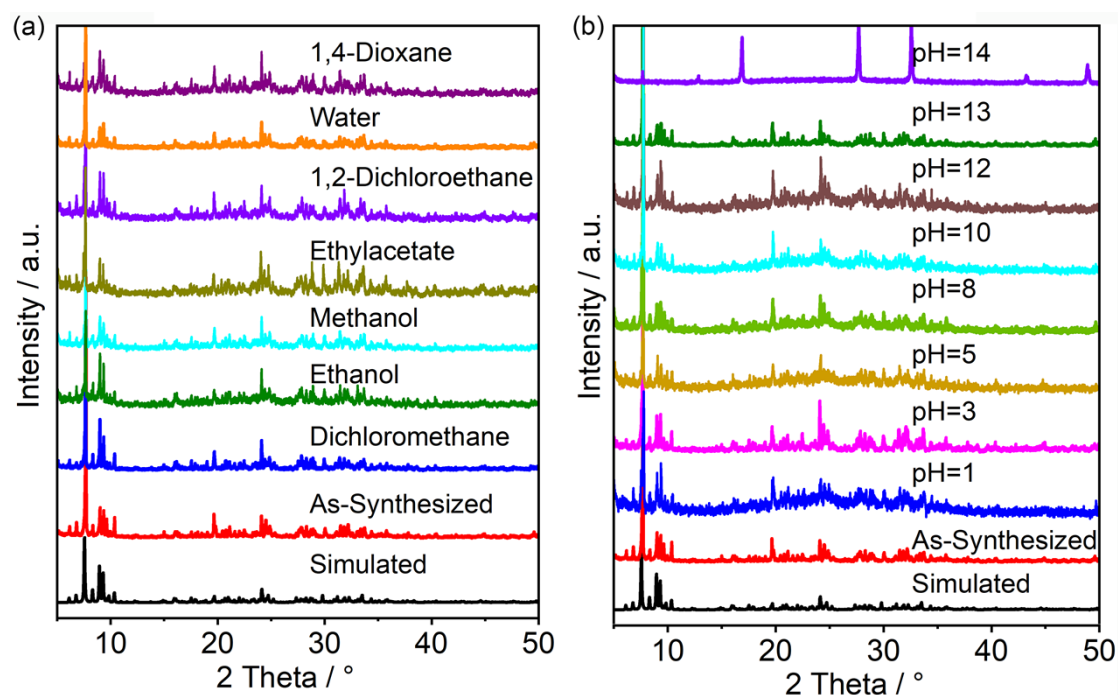


**Fig. S6** PXRD patterns of compound **Co-PW** after immersing in a series of common solvents for 7 days and in different acid/base solutions with a pH of 1–13.

**Stability.** Taking **Co-PW** as an example, the chemical stability of **Co-PW** was studied. At room temperature, the **Co-PW** was immersed in various common solvents (1, 4-dioxane, water, 1, 2-dichloroethane, ethylacetate, methanol, ethanol, dichloromethane) for 7 days and in different acid / base solutions with pH of 1–13 for 12h. The diffraction peaks of both experimental and simulated patterns match well, thus indicating that is no framework collapse or phase transition and the compound **Co-PW** possesses favorable solvent and acid / base stability (Fig. S6)

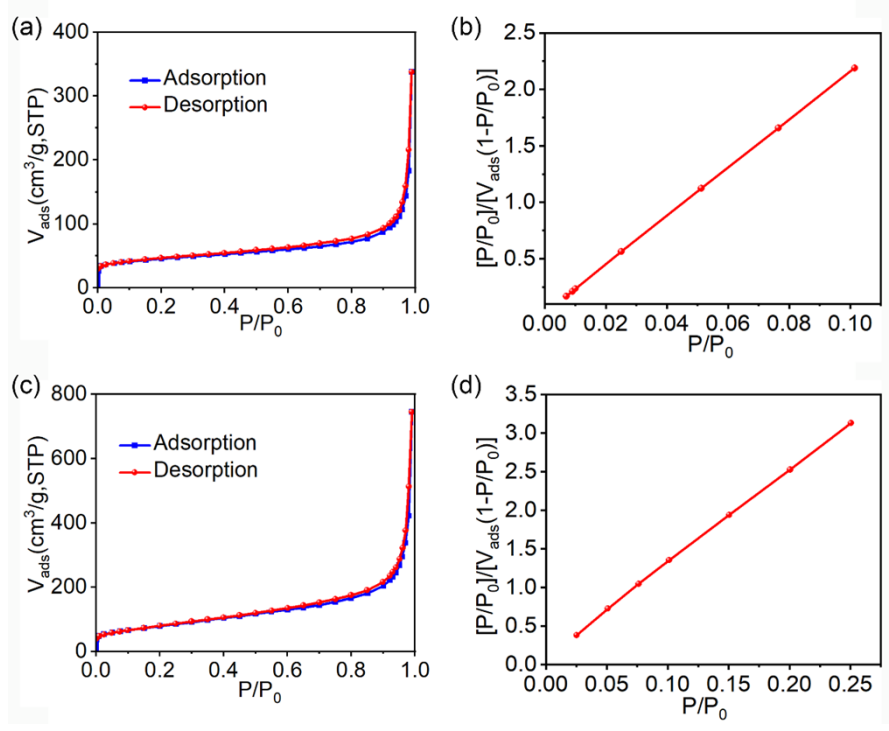


**Fig. S7.** BET analyses of compound **Co-PW** (a, b) and **Mn-PW** (c, d). The  $\text{N}_2$  absorption / desorption isotherms were measured at 77K ( $P_0 = 101$  kPa).

**BET analyses:** For a better dispersion in ACN, the **Co-PW** and **Mn-PW** crystals were ground and the Brunauer–Emmett–Teller (BET) surface area of **Co-PW** and **Mn-PW** were  $162.5 \text{ m}^2/\text{g}$  and  $284.9 \text{ m}^2/\text{g}$ .

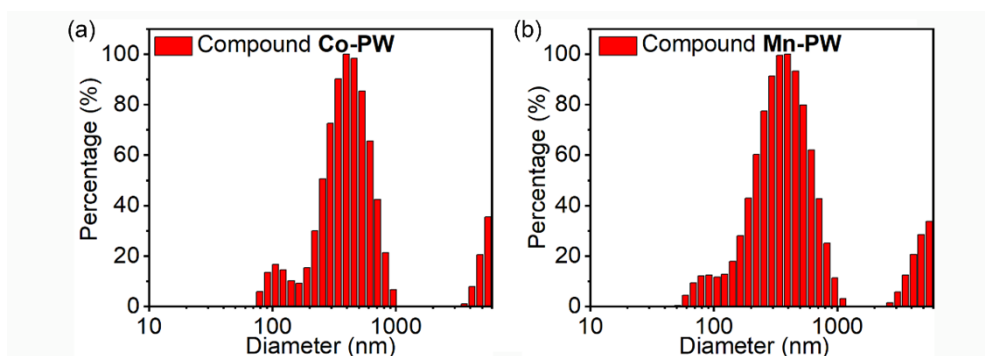


**Fig. S8.** DLS data for compounds **Co-PW** and **Mn-PW**.

**DLS analyses:** According to the result of dynamic light scattering (DLS), the hydrodynamic size of compounds **Co-PW** and **Mn-PW** were  $441.4 \text{ nm}$  and  $358.2 \text{ nm}$ .

**Table S6** Conversion and Selectivity of the Oxidation of Styrene to Styrene Oxide by compound **Co-PW** with O<sub>2</sub> as the Oxidant<sup>a</sup>.

Entry	Catal. (mg)	Solvent	Temp (°C)	Molar ratio of IBA / styrene	conv. <sup>b</sup> (%)	select. <sup>c</sup> (%)		
						styrene oxide	benzaldehyde	benzoic acid
1	20	Acetonitrile	25	2:1	18	50.1	49.9	
2	20	Acetonitrile	35	2:1	36	51.9	48.1	
3	20	Acetonitrile	45	2:1	66	48.3	51.7	
4	20	Acetonitrile	55	2:1	>99	92.6	7.4	
5	20	Acetonitrile	65	2:1	>99	80	14.8	5.2
6	10	Acetonitrile	55	2:1	88	84	16	
7	30	Acetonitrile	55	2:1	82.1	62.9	37	
8	20	1,2-Dichloroethane	55	2:1	56.5	80	20	
9	20	1,4-Dioxane	55	2:1	88.6	60.3	39.7	
10	20	Ethyl acetate	55	2:1	70.8	70.1	19.9	
11	20	Ethanol	55	2:1	20.6	100		
12	20	<i>n</i> -Octane	55	2:1	41.7	98	0.2	

<sup>a</sup>Reaction conditions: styrene (2 mmol), acetonitrile (5 mL) and O<sub>2</sub> 1 atm, IBA (4 mmol), reaction time, 2 hours.  
<sup>b,c</sup>Results determined by GC using biphenyl as internal standard.

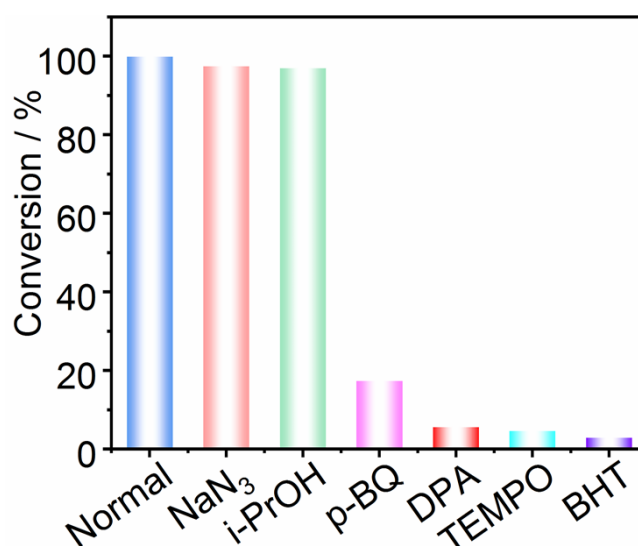


**Fig. S9** Styrene conversion over **Co-PW** in the presence of the different trapping species.

**Table S7** Comparison of different catalysts on styrene epoxidation<sup>a</sup>.

Entry	catalyst	T/°C	styrene/co-reductant ratio	Time/h	conversion/%	selectivity/%	TOF/h <sup>-1</sup>	Ref.
1	<b>Co-PW</b>	55	1:2	2	>99	92.6	167	This work
2	<b>Mn-PW</b>	55	1:2	2	84.6	83.5	141	This work
3	Cu-Imace-H-H][BF <sub>4</sub> ]	60	1:1	10	76	46	95	15
4	VO-Salen-SBA	80	1:2.5	8	78.6	71.2	63	16
5	FePcTs-Zn <sub>2</sub> Al-LDH	60	1:2.5	61	61	67	169	17
6	NENU-9N	45	1:2	5	97.2	93.5	156	18
7	FeP-CMP	25	1:3	24	55	69	23	19
8	Fe-salen-GO	80	1:2.5	8	76.5	49.8	175.5	20
9	[Cu <sub>3</sub> (BTC) <sub>2</sub> ]	40	1:2	6	58	58	5.7	21
10	IRMOF-3	40	1:2	6	52.3	80.7	4.9	22

<sup>a</sup> See the reference for the detailed structure of catalyst.

<sup>b</sup> Conversion of styrene.

<sup>c</sup> Selectivity of styrene oxide.

Turnover frequency (TOF) = (mol of styrene consumed) / (mol of the catalyst used × reaction time).

## References

1. J. C. Bailar Jr., H. S. Booth and M. Grennert, in *Inorg. Synth.*, 1939, vol. 1, pp. 132-133.
2. L. Krause, R. Herbst-Irmer, G. M. Sheldrick and D. Stalke, *J. Appl. Crystallogr.*, 2015, **48**, 3-10.
3. G. Sheldrick, *Acta Crystallogr. Sect. A*, 2008, **A64**, 112-122.
4. G. Sheldrick, *Acta Crystallographica Section C*, 2015, **71**, 3-8.
5. O. V. Dolomanov, L. J. Bourhis, R. J. Gildea, J. A. K. Howard and H. Puschmann, *J. Appl. Crystallogr.*, 2009, **42**, 339-341.
6. J. Sun, T. Zhou, D. Pan, X. Zhang, Y. Wang, Y.-C. Shi and H. Yu, *CrystEngComm*, 2020, **22**, 534-545.
7. X. Bai, X. Han, Y. Wang, A. Zhang, Y. Yang, Y. Lu and S. Liu, *Inorg. Chem.*, 2023, **62**, 13221-13229.
8. Q. Wang, B. Xu, Y. Wang, H. Wang, X. Hu, P. Ma, J. Niu and J. Wang, *Inorg. Chem.*, 2021, **60**, 7753-7761.
9. S.-M. Zhang, Y. Wang, Y.-Y. Ma, Z.-B. Li, J. Du and Z.-G. Han, *Inorg. Chem.*, 2022, **61**, 20596-20607.
10. Y. Chen, S. Chang, H. An, Y. Li, Q. Zhu, H. Luo and Y. Huang, *ACS Sustainable Chem. Eng.*, 2021, **9**, 15683-15693.
11. X. Liu, L. Cui, K. Yu, J. Lv, Y. Liu, Y. Ma and B. Zhou, *Inorg. Chem.*, 2021, **60**, 14072-14082.
12. M.-T. Li, X.-Y. Yang, J.-S. Li, N. Sheng, G.-D. Liu, J.-Q. Sha and Y.-Q. Lan, *Inorg. Chem.*, 2018, **57**, 3865-3872.
13. J.-Q. Sha, X.-Y. Yang, N. Sheng, G.-D. Liu, J.-S. Li and J.-B. Yang, *J. Solid State Chem.*, 2018, **263**, 52-59.
14. F.-r. Li, J.-h. Lv, K. Yu, M.-l. Zhang, K.-p. Wang, F.-x. Meng and B.-b. Zhou, *CrystEngComm*, 2018, **20**, 3522-3534.
15. G. Yang, H. Du, J. Liu, Z. Zhou, X. Hu and Z. Zhang, *Green Chem.*, 2017, **19**, 675-681.
16. Y. Yang, Y. Zhang, S. Hao, J. Guan, H. Ding, F. Shang, P. Qiu and Q. Kan, *Applied Catalysis A: General*, 2010, **381**, 274-281.
17. W. Zhou, J. Zhou, Y. Chen, A. Cui, F. a. Sun, M. He, Z. Xu and Q. Chen, *Applied Catalysis A: General*, 2017, **542**, 191-200.
18. Q. Yue, Y. Lu, Z. Zhang, H. Tian, H. Wang, X. Li and S. Liu, *New J. Chem.*, 2020, **44**, 16913-16920.
19. L. Chen, Y. Yang, Z. Guo and D. Jiang, *Adv. Mater.*, 2011, **23**, 3149-3154.
20. Z. Li, S. Wu, H. Ding, H. Lu, J. Liu, Q. Huo, J. Guan and Q. Kan, *New J. Chem.*, 2013, **37**, 4220-4229.
21. Y. Qi, Y. Luan, J. Yu, X. Peng and G. Wang, *Chem. Eur. J.*, 2015, **21**, 1589-1597.
22. S. Bhattacharjee, D.-A. Yang and W.-S. Ahn, *Chem. Commun.*, 2011, **47**, 3637-3639.